Segregation of voids in a spatially heterogeneous dislocation microstructure

S. L. Dudarev*
EURATOM/UKAEA Fusion Association, Culham Science Centre, Oxfordshire OX14 3DB, United Kingdom

A. A. Semenov and C. H. Woo
Department of Electronic and Information Engineering, Polytechnic University of Hong-Kong, Hung Hom, Kowloon, Hong-Kong
(Received 20 February 2004; published 29 September 2004)

We investigate the dynamics of nucleation and the growth of voids in an irradiated material in the presence of a spatially heterogeneous dislocation microstructure. We find that, due to the sensitivity of the void nucleation rate to the local vacancy supersaturation, voids nucleate and grow almost exclusively in the regions where the density of dislocations is low. Numerical simulations show that the relatively high void growth rates observed experimentally in the regions of low dislocation density, leading to segregated evolution of dislocations and voids, can be naturally described by solutions of a spatially heterogeneous reaction-diffusion model that takes continuous nucleation of voids into account but does not assume the occurrence of long-range one-dimensional transport of clusters of self-interstitial atoms through the material.

DOI: 10.1103/PhysRevB.70.094115 PACS number(s): 61.72.Mm, 61.80.Az, 61.82.Bg, 28.52.Fa

I. INTRODUCTION

The development of materials suitable for the construction of a commercial fusion power plant is one of the main technical tasks in the realization of nuclear fusion as an economically viable alternative to the use of fossil fuels.[1–3] Given a broad range of challenging issues associated with the empirical testing of candidate materials in a simulated fusion environment,[1,4] modeling the microstructural evolution of materials has become a significant part of the international fusion development program.[5,6]

The kinetics of phase transformations in materials driven far from equilibrium by irradiation is characterized by the dynamic balance between the creation of lattice defects and their annihilation at dislocations, grain boundaries, or other elements of the microstructure, and through clustering. The development of a unified fully quantitative mathematical treatment of microstructural evolution of a material is hindered by the presence of highly disparate time and length scales characterizing this evolution.[5,6] Also, the extent to which this evolution can be adequately described by an effective spatially averaged homogeneous model has long remained a subject of debate. The original formulation of the reaction-diffusion "standard rate" theory[7,8] assumed a spatially homogeneous and time-independent concentration of diffusing point defects, and a homogeneous distribution of sinks for these defects. The connection between this model and the actual heterogeneous microstructure of materials was made through the effective medium approximation investigated by Brailfsord[9] and, more recently, by Doan and Martin.[10]

At the same time in many cases the spatial heterogeneity of the material represents the main factor determining the mode of microstructural evolution. One example of this is given by the behavior of nanocrystalline materials under irradiation,[11,12] where a high concentration of grain boundaries has a strong effect on the development of collision cascades. Another striking effect is the spatially segregated void swelling observed in several materials at low irradiation doses.[13–15] In this case voids form predominantly in the regions of low density of dislocations, in a seemingly apparent contradiction with the reaction-diffusion standard rate theory model[7] in which the growth of voids is driven by the preferential absorption of interstitial atoms by dislocations. Furthermore, spatially heterogeneous materials, like complex steels or nanocomposite oxide-metal systems are presently considered to be among the most promising candidates for fusion and advanced fission applications in view of their ability to trap helium at interfaces and to sustain high levels of irradiation damage.[16]

A current interpretation of the observed effects is based on the concept of one-dimensional Brownian motion of self-interstitial atom clusters.[17–19] In the case of a nanocrystalline material molecular dynamics simulations show the one-dimensional migration of clusters in the stress field of grain boundaries occurring on the ten-nanometer scale.[20] In the case of spatially segregated void swelling[13–15] the failure of the reaction-diffusion models investigated by Leffers *et al.*[21] to explain experimental observations has led to the hypothesis that it is the occurrence of the *long-range* one-dimensional transport of self-interstitial clusters through the material on the scale exceeding several thousand nanometers[22] that is responsible for the segregated growth of voids between the dislocation walls.

However, *in-situ* electron microscope observations of the motion of defects in irradiated specimens[23,24] have not so far confirmed the actual occurrence of the long-range transport of interstitial atom clusters. Instead, these observations point to the possibly significant part played by thermal excitations giving rise to random changes in the direction of motion of clusters or interaction with trapping centers in the bulk of the material[25] that hinder the one-dimensional diffusion of clusters and enhance the three-dimensional character of their motion.[26,27]

This poses two significant questions: namely, (i) in the absence of *long-range* one-dimensional transport, what is the possible mechanism that drives the nucleation and growth of voids spatially segregated from dislocations, and (ii) how can

 ©2004 The American Physical Society

we explain the observed evolution in view of its relatively large spatial scale (a thousand nanometers)? We show that both questions can be resolved within a relatively simple reaction-diffusion type model that takes into account the nucleation of voids in collision cascades. The point that the nucleation aspect of the problem is important follows from the fact that all the experimental observations of heterogeneous microstructures[13–15] refer to the initial stage of microstructural evolution (low irradiation doses) where nucleation and the growth of voids occur continuously and simultaneously. Although the significance of continuous nucleation is clearly evident from observations, it has not been included in the models considered so far.[21,22] A new treatment of nucleation developed in Ref. 28 has simplified the problem to the extent that we can now apply it to the investigation of a sufficiently general but still tractable spatially heterogeneous case.

In this paper we examine a sufficiently general diffusion-reaction-nucleation model of an irradiated material characterised by a spatially heterogeneous dislocation microstructure. We find that a combined treatment of nucleation and growth of voids can explain very well a segregated occurrence of voids between dislocation walls similar to that observed experimentally. Numerical solutions obtained for the relevant range of parameters[13–15] are in agreement with observations. These findings suggest that the observed effects may be explained without assuming the presence of long-range one-dimensional transport of interstitial defect clusters, which was previously believed[22] to represent an essential part of the treatment of the problem.

We start by showing that in the case where continuous void nucleation is not explicitly taken into account[21] the solutions do not match experimental observations. We then investigate a spatially heterogeneous reaction-diffusion model that includes the treatment of continuous nucleation and show that in this case the predicted picture of microstructural evolution agrees much better with experimental findings. We conclude by assessing the limits of validity of the model.

II. THE LEFFERS MODEL

We start by investigating a model that describes growth of voids in the presence of a pre-existing spatially heterogeneous dislocation microstructure. We assume that all the voids are instantly nucleated at the initial moment of time $t=0$ and that the subsequent microstructural evolution only involves the *growth* of voids driven by the supersaturation of vacancies in the material. A simplified version of this model (where instead of following the integral history of microstructural evolution the authors treated a few "snapshots" describing an assumed state of the material at a certain dose) was first considered by Leffers *et al.*[21] In what follows for convenience we refer to it as to the Leffers model. The rate of change of the radius $a(\mathbf{r},t)$ of a void situated at point $\mathbf{r}$ in the material is proportional to the vacancy supersaturation $D_v c_v(\mathbf{r},t) - D_i c_i(\mathbf{r},t)$ at that point,[7]

$$da(\mathbf{r},t)/dt = [D_v c_v(\mathbf{r},t) - D_i c_i(\mathbf{r},t) - D_v C_s(a)]/a(\mathbf{r},t), \quad (1)$$

where D_v and D_i are the diffusion coefficients of vacancies and interstitial atoms, and $c_v(\mathbf{r},t)$ and $c_i(\mathbf{r},t)$ are the local concentrations of these two types of defects. In Eq. (1) the term $D_v C_s(a)$ describes thermal evaporation of vacancies. For the supercritical voids in the range of parameters relevant to experimental observations[13–15] this term does not have an appreciable effect on the growth rate and in what follows it will be neglected. In the case where the clustering of interstitial atoms in collision cascades plays a significant part,[29] parameters D_i and c_i represent effective quantities that describe the total flux of interstitial atoms and include contributions of both single interstitial atoms and interstitial atoms clusters performing a three-dimensional random walk in the material.[26,27] In the limit of low irradiation rates where the recombination of vacancy and interstitial defects in binary collisions may be neglected, concentrations c_v and c_i satisfy the system of two equations:

$$D_\alpha \nabla^2 c_\alpha(\mathbf{r},t) + K(1-\epsilon_r) - [Z_\alpha \rho(\mathbf{r}) + 4\pi N a(\mathbf{r},t)] D_\alpha c_\alpha(\mathbf{r},t) = 0, \quad (2)$$

where the index α refers to either vacancies ($\alpha = v$) or interstitial type defects ($\alpha = i$). In this equation $\rho(\mathbf{r})$ is the volume density of edge dislocations, Z_α are the dislocation bias factors ($Z_i > Z_v$), and $N(\mathbf{r})$ is the volume density of voids. In the Leffers model $N(\mathbf{r})$ is assumed to be constant as a function of time and is a globally averaged quantity independent of the coordinate $\mathbf{r}$. Concentrations $c_\alpha(\mathbf{r},t)$ depend on time t in a self-consistent way via $a(\mathbf{r},t)$ given by Eq. (1) To model a spatially heterogeneous microstructure the density of dislocations was modulated in the direction of the x-axis in the form of dislocation walls, as shown in Fig. 1. We postpone the discussion of the numerical treatment until the next section and begin by considering the solutions of the above equations.

The profiles shown in Fig. 1 are qualitatively similar to those shown in Fig. 2 of Ref. 21. The main feature of the predicted spatial distribution of vacancy supersaturation illustrated in Fig. 1 is the presence of pronounced peaks near the dislocation walls. It is this feature of the solution of the Leffers model[21] that does not agree with experimental findings reported in Refs. 13–15. In experiments voids form almost exclusively in the space between the dislocation walls and almost no voids are observed in the immediate vicinity of the walls, while the profile of vacancy supersaturation shown in Fig. 1 suggests that voids should be expected to grow at the fastest rate near the walls. It is this qualitative difference between the solutions of the Leffers model and experimental observations that stimulated the hypothesis that the formation of the observed void swelling profiles was driven by some unusual mode of transport of interstitial atoms involving long-range one-dimensional diffusion.[22]

III. SPATIALLY HETEROGENEOUS REACTION-DIFFUSION-NUCLEATION MODEL

We now consider how the solutions of a reaction-diffusion model change if the continuous nucleation of voids is taken

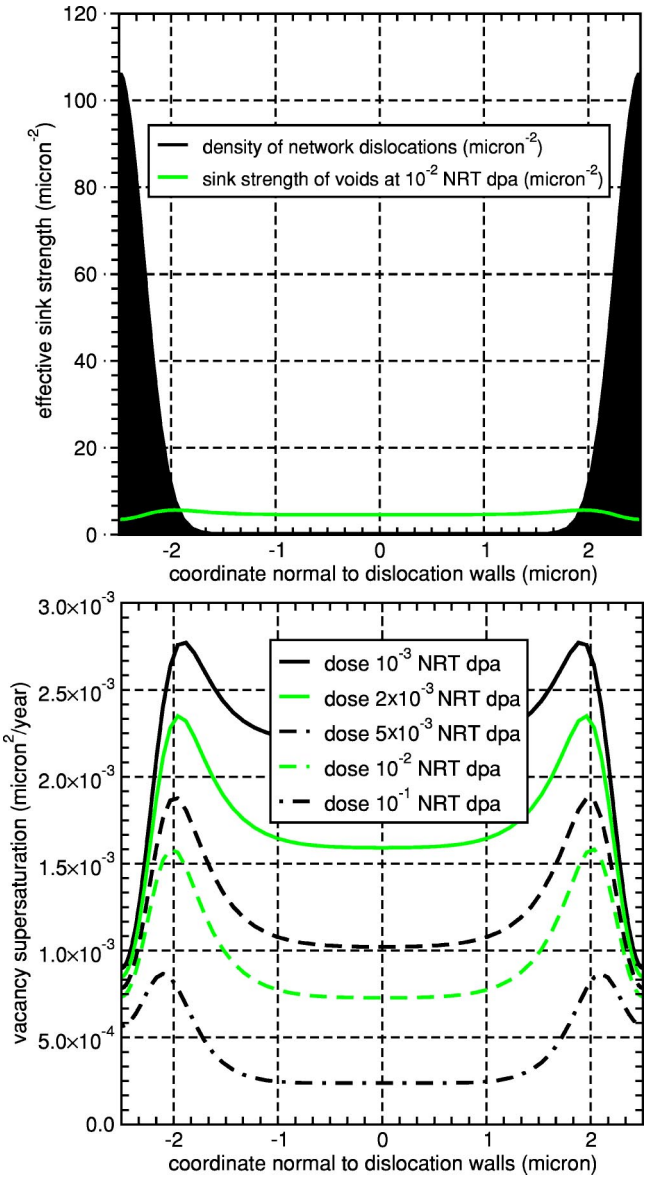

FIG. 1. (Color online) (Top) Spatial distribution of the network density of dislocations $\rho(x)$ used in calculations, and the profile of the sink strength $4\pi Na(x,t)$ of voids. (Bottom) Profile of vacancy supersaturation $D_v c_v(x,t) - D_i c_i(x,t)$ evaluated using the Leffers model for $\phi = Kt = 10^{-2}$ NRT dpa assuming that the volume density of voids equals $N = 10^{20}$ m^{-3}. The dose rate K equals $K = 2$ NRT dpa/year, $Z_i = 1.15$, $Z_v = 1.0$.

into account in a self-consistent manner. Let $\nu(\mathbf{r},t)$ be the rate of nucleation of voids normalized by the condition

$$\int_0^t \nu(\mathbf{r},\tau)d\tau = N(\mathbf{r},t), \tag{3}$$

where $N(\mathbf{r},t)$ is the local density of voids at point $\mathbf{r}$ at time t. The local void swelling is defined as

$$S(\mathbf{r},t) = \frac{4}{3}\pi \int_0^t \nu(\mathbf{r},\tau)a^3(\mathbf{r},t,\tau)d\tau, \tag{4}$$

where $a(\mathbf{r},t,\tau)$ is the radius of a void nucleated at the moment $t=\tau$. By differentiating (4) we find the following expression for the swelling rate:

$$\frac{dS(\mathbf{r},t)}{dt} = 4\pi \int_0^t \nu(\mathbf{r},\tau)a^2(\mathbf{r},t,\tau)\frac{da(\mathbf{r},t,\tau)}{dt}d\tau + \frac{4}{3}\pi\nu(\mathbf{r},t)a^3(\mathbf{r},t,t), \tag{5}$$

where in most cases the last term can be neglected since the critical radius of nucleating voids $a(\mathbf{r},t,t)$ is small in comparison with the average radius of voids already formed and growing in material. In the presence of continuously occurring nucleation the evolution of an ensemble of voids can be described by a system of equations similar to (1) and (2), namely

$$\frac{da(\mathbf{r},t,\tau)}{dt} = \frac{\Theta(t-\tau)}{a(\mathbf{r},t,\tau)}[D_v c_v(\mathbf{r},t) - D_i c_i(\mathbf{r},t)], \tag{6}$$

and

$$D_\alpha \nabla^2 c_\alpha(\mathbf{r},t) + K(1-\epsilon_r) - \left[Z_\alpha \rho(\mathbf{r}) + 4\pi \int_0^t \nu(\mathbf{r},\tau)a(\mathbf{r},t,\tau)d\tau\right] D_\alpha c_\alpha(\mathbf{r},t) = 0, \tag{7}$$

where $\Theta(t-\tau)=1$ for $t>\tau$ and $\Theta(t-\tau)=0$ for $t<\tau$, and $\epsilon_r \sim 80\%$ is the fraction of defects recombining directly in collision cascades.

Equations (4)–(7) can be integrated using the supercell method similar to that used in large-scale electronic structure calculations[30] and in the treatment of electron diffraction.[31] Consider the diffusion of particles in the presence of a spatially heterogeneous distribution of sinks,

$$\nabla^2 \Pi(\mathbf{r}) - \Omega(\mathbf{r})\Pi(\mathbf{r}) + K(1-\epsilon_r) = 0. \tag{8}$$

Here $\Pi(\mathbf{r},t) = \Pi(\mathbf{r}) = D_\alpha c_\alpha(\mathbf{r},t)$ is a potential function, the gradient of which gives the local flux of mobile defects, and $\Omega(\mathbf{r}) = \Omega(\mathbf{r},t) = Z\rho(\mathbf{r}) + 4\pi\int_0^t \nu(\mathbf{r},\tau)a(\mathbf{r},t,\tau)d\tau$ is the local density of sinks. Representing $\Omega(\mathbf{r})$ and the potential function $\Pi(\mathbf{r})$ in the form of a Fourier series,

$$\Pi(\mathbf{r}) = \sum_{\mathbf{g}} \Pi_{\mathbf{g}} \exp(i\mathbf{g}\cdot\mathbf{r}),$$

$$\Omega(\mathbf{r}) = \sum_{\mathbf{g}} \Omega_{\mathbf{g}} \exp(i\mathbf{g}\cdot\mathbf{r}), \tag{9}$$

we write Eq. (8) as

$$\sum_{\mathbf{g}'} (\mathbf{g}'^2 \delta_{\mathbf{g}\mathbf{g}'} + \Omega_{\mathbf{g}-\mathbf{g}'}) \Pi_{\mathbf{g}'} = K(1-\epsilon_r)\delta_{\mathbf{g}0}. \quad (10)$$

The matrix $\mathbf{g}^2\hat{I}+\hat{\Omega}$ entering this equation is Hermitian, and it can therefore be diagonalized by a unitary transformation,

$$\sum_{\mathbf{g},\mathbf{g}'} (U^{\dagger})_{j\mathbf{g}} (\mathbf{g}'^2 \delta_{\mathbf{g}\mathbf{g}'} + \Omega_{\mathbf{g}-\mathbf{g}'}) U_{\mathbf{g}'j'} = \omega_j \delta_{jj'}, \quad (11)$$

where ω_j are the eigenvalues corresponding to eigenvectors $U_{\mathbf{g}j}$. Using the property of orthogonality of eigenvectors of a Hermitian matrix,

$$\sum_{\mathbf{g}} (U^{\dagger})_{j\mathbf{g}} U_{\mathbf{g}j'} = \delta_{jj'}, \quad (12)$$

we find the solution of Eq. (10),

$$\Pi_{\mathbf{g}} = K(1-\epsilon_r) \sum_j \frac{U_{\mathbf{g}j}(U^{\dagger})_{j0}}{\omega_j}. \quad (13)$$

Assuming that the density of dislocations is described by a "Kronig-Penney"-type function $\rho(x)$ defined as $\rho(x)=\rho_w$ inside the walls and $\rho(x)=\rho_{bg} \ll \rho_w$ in the space between the walls, we find the Fourier components ρ_g as

$$\rho_g = \rho_{bg}\delta_{no} - \frac{\rho_w}{\pi n} \sin\left[\pi n\left(1-\frac{l}{L}\right)\right] \exp(-\lambda n^2). \quad (14)$$

Here L is the period of the dislocations walls structure, $g=2n\pi/L$ is a reciprocal lattice vector, l is the width of the walls, and $\lambda \ll 1$ is a damping factor. In all the calculations described below we assumed that $\rho_w = 10^{14}$ m^{-2} and $\rho_{bg} = 0.01\rho_w = 10^{12}$ m^{-2} (the choice of the latter value is significant, and we discuss this point in greater detail below). The time integration of the reaction-diffusion equations typically involves several thousand steps, where at each step the Fourier components of the total density of sinks $\Omega_g(t)$ are updated using the information accumulated over the entire preceding interval of time $0<\tau<t$. Spatial integration was performed using 64-point Gaussian quadratures.[32] The value of the dislocation bias factor Z_i was chosen to be 1.30 in agreement with the calculated values for copper.[33] Although this 30% bias value is somewhat larger than the value used by Leffers *et al.*,[21] it is still significantly lower than the extreme 200% value of bias also considered in Ref. 21 in an attempt to improve the agreement between the model and experimental observations. We note that the choice of a relatively large 30% bias factor is consistent with the assumption that the transport of interstitial atoms also involves the diffusion of interstitial atom clusters that interact with dislocations stronger than single interstitial atoms.

The accuracy of numerical integration of Eqs. (6)–(13) was verified using the global conservation law,

$$\frac{d}{dt}\left[\int_V S(\mathbf{r},t)d^3r\right] = \int_V \rho(\mathbf{r})[Z_i D_i c_i(\mathbf{r},t) - Z_v D_v c_v(\mathbf{r},t)]d^3r, \quad (15)$$

derived in Appendix I. The expression for the rate of the nucleation of voids $\nu(\mathbf{r},t)$ used in this work was taken from Ref. 28, and is given by $\nu=K(1-\epsilon_r)P/N_d$, where N_d is the average number of defects produced in a single collision cascade and P is the probability of void nucleation given in Appendix II. In terms of our model, the most significant feature of the void nucleation probability is its high sensitivity to the local vacancy supersaturation.

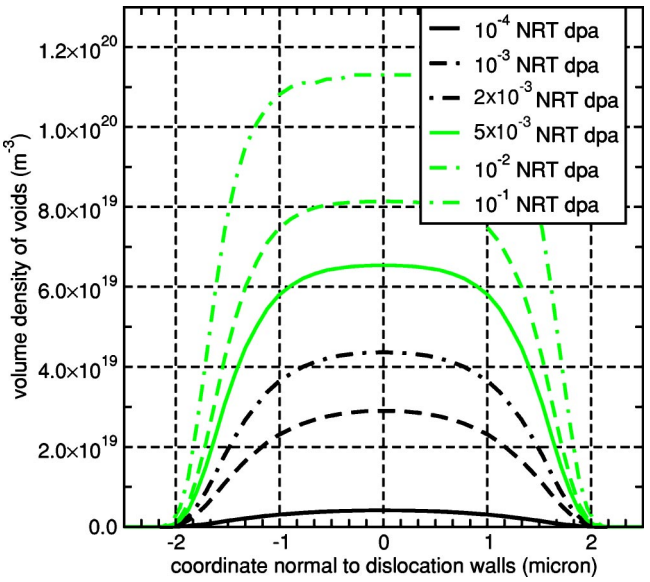

FIG. 2. (Color online) Volume density of voids shown as a function of coordinate x in the direction normal to dislocation walls for several values of the irradiation dose $\phi=Kt$ (in units of NRT dpa). Calculations were performed for $K=2$ NRT dpa/year, $\gamma_s = 1.4$ J/m^2, $Z_i=1.3$, $Z_v=1.0$, $1-\epsilon_r=0.2$, and $N_d=50$.

Figure 2 shows how the density of voids $N(x,t)$ nucleated at various points in the simulation cell increases as a function of the irradiation dose. In contrast to the findings of the Leffers model,[21] profiles shown in Fig. 2 follow the trend similar to that found experimentally in Refs. 13–15. For example, the sketch shown in Fig. 1 of Ref. 13 shows that voids were distributed almost homogeneously in the space between the dislocation walls, while the density of voids was significantly reduced in the immediate vicinity of the walls. The calculated profiles of the density of voids shown in Fig. 2 exhibit 0.5 micron-wide void denuded zones adjacent to dislocation walls. In these zones the density of voids is reduced by more than an order of magnitude in comparison with the density of voids in the space between the walls. Inside the dislocation walls the predicted density of voids is exceedingly low, and this also agrees with experimental observations. Another interesting feature characterizing the evolution of voids occurring in the presence of dislocation walls is the uneven distribution of the average size of voids. Larger voids form in the space between the dislocation walls, and the experimentally measured average diameter of voids decreases by approximately 30% in the zone adjacent to the walls. The calculated spatial distributions of the average diameter of voids are shown in Fig. 3. The average diameter of voids decreases by almost 50% inside the dislocation walls in comparison with voids situated in the space between the walls, where the density of dislocations is low. Another significant parameter characterizing the evolution of the microstructure is the void

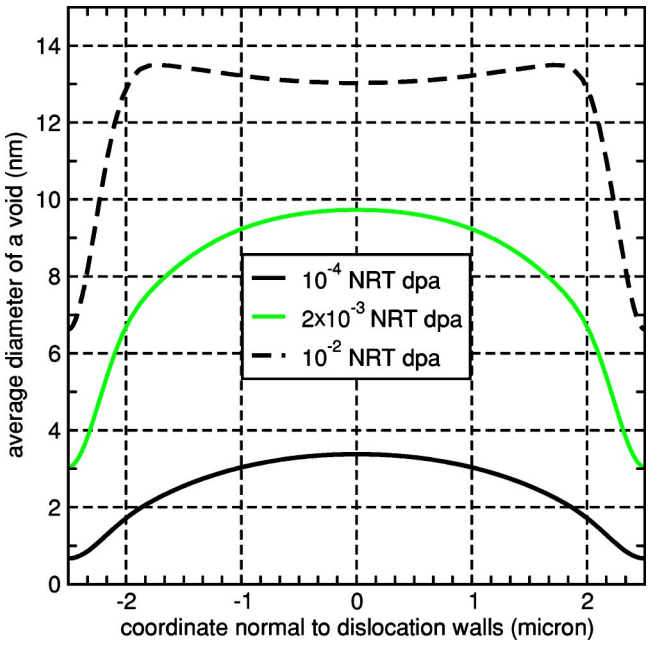

FIG. 3. (Color online) The average diameter $\overline{d}(x,t)$ of a void defined as $\overline{d}(x,t)=[6S(x,t)/\pi N(x,t)]^{1/3}$, where $S(x,t)$ is the local void swelling, shown as function of coordinate x in the direction normal to dislocation walls. Parameters used in the calculations are the same as in Fig. 2. Note that the density of voids near the dislocation walls is very low, and this agrees with the fact that no voids were experimentally observed in the walls (Ref. 13), despite the fact that the void *size* criterion suggests that they might still be detected.

swelling *rate* defined as the ratio of the local volume swelling $S(x,t)$ to the irradiation dose Kt. Experimental observations reported in Refs. 13–15 showed that this rate approached 2% per Norgett-Robinson-Torrens[34] (NRT) displacements per atom (dpa) units, and the Leffers model[21] encountered difficulties in trying to explain this relatively high value. Figure 4 shows profiles of the swelling rate evaluated using the reaction-diffusion-nucleation model described above. For $Kt<10^{-2}$ NRT dpa the profiles of the function $S(x,t)/Kt$ are maximum in the center of the simulation cell, and the calculated swelling rate in the interval of doses $2\times10^{-3}<Kt<10^{-2}$ is close to 1% per NRT dpa in reasonable agreement with the rate observed experimentally. In the large dose limit the model exhibits the formation of peaks of swelling in the vicinity of dislocation walls. Similar peaks are known to occur in other spatially heterogeneous microstructures, for example, in the vicinity of grain boundaries.[26] Experimental observations addressing the low dose limit[13–15] do not show the development of peak swelling zones near dislocation walls. Here we note that in contrast to the case of grain boundaries, dislocation walls neither have ideal planar geometry nor do they retain stability in the limit of a larger irradiation dose. Both of these factors impede the development of zones of enhanced swelling shown in Fig. 4 for $Kt=10^{-1}$ NRT dpa.

IV. DISCUSSION

The study of solutions of the reaction-diffusion-nucleation model described above shows that the model reproduces

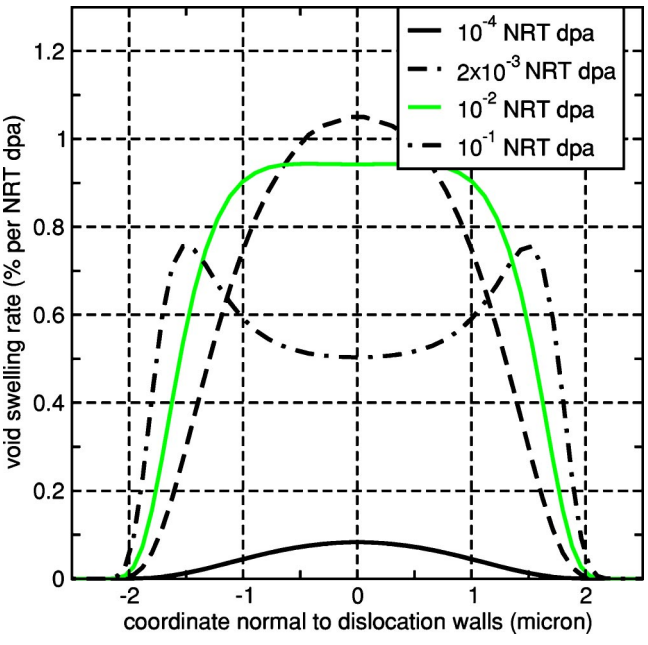

FIG. 4. (Color online) The void swelling rate $S(x,t)/Kt$ plotted as a function of coordinate x for several values of irradiation dose. Parameters used in the calculation are the same as in Fig. 2.

practically all the significant features characterizing the experimentally observed evolution of an ensemble of voids nucleating and growing in the presence of a heterogeneous dislocation microstructure. The inclusion of continuously occurring void nucleation in the model, as well as the full treatment of spatial and temporal evolution of the void component of the microstructure, are the main points that make our treatment different from the treatment of models considered

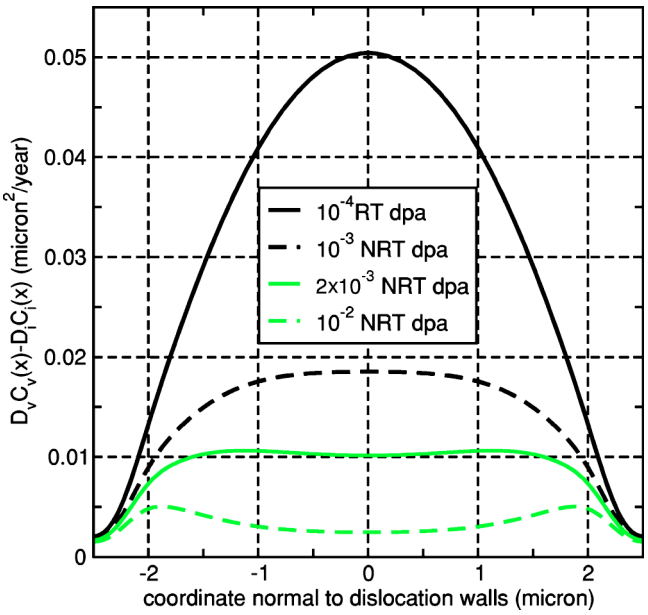

FIG. 5. (Color online) Profiles of vacancy supersaturation $D_v c_v(x,t)-D_i c_i(x,t)$ shown as a function of coordinate x for several values of the irradiation dose. Calculations were carried out for the same set of parameters as that given in the caption to Fig. 2.

previously.[21] As we have already noted above, the rate of nucleation of voids is a function that is sensitive to the local level of vacancy supersaturation. The evolution of profiles of vacancy supersaturation shown in Fig. 5 explains why we find that in the limit of low dose voids nucleate predominantly in the space between the dislocation walls. Both the numerical solutions and analytical estimates show that up to the dose of the order of 2×10^{-3} NRT dpa vacancy supersaturation is maximum between the dislocation walls, and it is there where experimental observations show the formation of regions with the highest density of voids. Another significant point that requires consideration refers to the origin of the dislocation walls themselves. In our model, as well as in the earlier approaches,[21] it was assumed that dislocation microstructure remained stationary during the entire interval of evolution of the system. In experiments dislocation walls appeared relatively early during irradiation (reportedly they were present already at the lowest dose $Kt=2\times10^{-3}$ NRT dpa investigated in Refs. 13–15) and then they vanished as the dose increased. The latter effect can be readily understood if we estimate the distance climbed by dislocations at various points in the simulation cell,

$$X_c(x)=\frac{1}{b}\int_0^t [Z_iD_ic_i(x,\tau)-Z_vD_vc_v(x,\tau)]d\tau, \qquad (16)$$

where b is the magnitude of the Burgers vector of a dislocation. As the dose reaches $Kt=10^{-1}$ NRT dpa the value of $|X_c(x)|$ approaches 2.5 microns in the space between the dislocation walls and 0.08 microns inside the walls. These values are comparable with the spatial scale characterizing the heterogeneity of the dislocation microstructure itself (see Fig. 1). This estimate showing that the heterogeneous dislocation microstructure "melts" at $Kt\sim0.1$ NRT dpa explains the absence of dislocation walls in specimens irradiated to higher doses. On the other hand, the origin of formation of dislocation walls in the material in the limit of low doses requires investigating the collective behavior of dislocations. The emergence of symmetry broken solutions in the equations describing interacting dislocations, dislocation loops, and mobile defects may, in our view, be the most likely mechanism responsible for the formation of dislocation walls.[35,36] In particular, solutions described in Refs. 35 and 36 show that immobile small dislocation loops are eliminated in the space between the dislocation walls, leading to the formation of a heterogeneous distribution of network dislocations similar to the one assumed in our model. The fact that the dislocation walls form at an early stage of irradiation where the density of voids is still relatively low[13] shows that the assumption that the heterogeneous distribution of the density of dislocations remains stationary within the interval of doses considered in this study represents a viable approximation.

A new set of experimental observations related to our model was performed recently by Singh *et al.*[37] In this work the authors compared void microstructures generated in copper by electron, proton, and neutron irradiation. The material studied in Ref. 37 was several times less pure than that investigated in Ref. 13, and it contained 30 times more oxygen than copper used in similar experiments performed by English *et al.*[14] This may explain the fact that the density of voids observed in Ref. 37 at $Kt=10^{-2}$ NRT dpa was approximately ten times higher than that reported in Ref. 13. Bearing in mind that the expression for the nucleation rate derived in Ref. 28 and Appendix II does not take the impurity effect into account, we do not compare our calculations with the neutron data reported in Ref. 37. Still, it is instructive to assess the new data in connection with the analysis given above.

Two aspects need to be taken into account in the comparison of effects of charge particle and neutron irradiation. In the case of irradiation by charged particles a significant number of atoms is displaced through large impact parameter collisions giving rise to either smaller cascades (in the case of protons) or to the generation of individual Frenkel pairs (in the case of electrons). This affects the rate of nucleation of voids since, for example, in the case of electron irradiation nucleation of voids is suppressed due to the difficulty of accumulating a critical number of vacancies in a vacancy cluster through a sequence of binary interactions of vacancies with the cluster. In the treatment of void nucleation adopted in this paper, relatively large nuclei for the thermally stable supercritical voids are formed from vacancy clusters formed directly in collision cascades. In the case of electron irradiation there are no cascades, and void nucleation takes place through the sequential agglomeration of single vacancies. The probability of nucleating a void in this case is much lower that in the case of cascade nucleation. Therefore in the limit of low dose and electron irradiation the void number density is expected to be significantly lower than in the case of proton or neutron irradiation corresponding to the same dose. Proton irradiation, in addition to Frenkel pairs, produces a significant number of small cascades, and voids nucleate at the rate intermediate between that of electron and neutron cases.[37]

In addition to the difference in the void nucleation rates, the interstitial component of the microstructure is also strongly affected by the cascade nature of the nucleation process. The formation of larger clusters in the case of neutron irradiation facilitates the formation of interstitial clusters and mesoscopic dislocation loops. Using the neutron irradiation data from Ref. 14 we estimate that dislocation loops with the average radius of 1.2 nm distributed with the volume density of $N=3\times10^{20}$ m^{-3} contribute approximately 10^{12} m^{-2} to the average dislocation density of the material. It is this value that we use as an esimate for the effective density of dislocations in the space between the dislocation walls shown in Fig. 1. In the case of proton irradiation not only do the walls not form but also the effective density of dislocations remains low ($\sim10^{11}$ m^{-2}), giving rise to low swelling. Our calculations show that the density of voids in this case reaches early saturation and remains nearly constant over the entire interval of doses investigated experimentally, in agreement with experimental results reported in Ref. 37.

Summarizing the main points of our analysis, we conclude that a model describing the nucleation of voids in the material, the reaction of defects with a heterogeneous dislocation microstructure, and the three-dimensional diffusion of

defects in the material can reproduce at a reasonable level of accuracy some of the main qualitative features characterizing the experimentally observed picture of microstructural evolution. In our model we did not assume the occurrence of long-range one-dimensional transport of interstitial defects on the several thousand nanometers length scale, and still arrived at a reasonably accurate mathematical model of the observed phenomena. This shows that the hypothesis about the significant part played by *long-range* one-dimensional transport of defects remains an interesting, but yet unconfirmed, proposition that requires experimental verification of a more direct nature than that given by the interpretation of features of evolution of a spatially heterogeneous microstructure.

ACKNOWLEDGMENTS

This work was performed as a part of a collaboration on modeling fusion materials between the EURATOM/UKAEA Fusion Association and the Hong-Kong Polytechnic University. Work at the Hong-Kong Polytechnic University was supported by Grants No. PolyU5167/01E and No. PolyU5173/01E from the Research Grant Council of Hong Kong. Work at the UKAEA Culham Science Centre was supported by the UK Engineering and Physical Sciences Research Council (EPSRC) and by EURATOM. We are grateful to R. Bullough and A. P. Sutton for stimulating discussions We also thank I. Cook and J. W. Connor for their encouragement and comments.

APPENDIX A: THE GLOBAL CONSERVATION LAW

To derive the *global* law of conservation of the total number of vacancies and interstitial atoms in an evolving heterogeneous microstructure we consider a system of two equations of the form

$$D_i\nabla^2 c_i(\mathbf{r},t) + K(1-\epsilon_r) - \left[Z_i\rho(\mathbf{r}) + 4\pi\int_0^t \nu(\mathbf{r},\tau)a(\mathbf{r},t,\tau)d\tau \right] D_i c_i(\mathbf{r},t) = 0,$$

$$D_v\nabla^2 c_v(\mathbf{r},t) + K(1-\epsilon_r) - \left[Z_v\rho(\mathbf{r}) + 4\pi\int_0^t \nu(\mathbf{r},\tau)a(\mathbf{r},t,\tau)d\tau \right] D_v c_v(\mathbf{r},t) = 0. \tag{A1}$$

By subtracting the second equation from the first one, and by integrating the result over the volume of the simulation cell we arrive at

$$\int_V [Z_i\rho(\mathbf{r})c_i(\mathbf{r},t)D_i - Z_v\rho(\mathbf{r})c_v(\mathbf{r},t)D_v]d^3r = 4\pi\int_V \left[\int_0^t d\tau\nu(\mathbf{r},\tau)a(\mathbf{r},t,\tau)c_v(\mathbf{r},t)D_v - \int_0^t d\tau\nu(\mathbf{r},\tau)a(\mathbf{r},t,\tau)c_i(\mathbf{r},t)D_i \right] d^3r. \tag{A2}$$

Taking into account the fact that

$$c_v(\mathbf{r},t)D_v - c_i(\mathbf{r},t)D_i = a(\mathbf{r},t,\tau)\frac{da(\mathbf{r},t,\tau)}{dt}, \tag{A3}$$

and combining this with Eq. (5), we find

$$\int_V \frac{dS(\mathbf{r},t)}{dt}d^3r = \int_V [Z_i\rho(\mathbf{r})c_i(\mathbf{r},t)D_i - Z_v\rho(\mathbf{r})c_v(\mathbf{r},t)D_v]d^3r. \tag{A4}$$

By transposing the operations of differentiation and integration on the left-hand side of this expression we arrive at the conservation law (15).

APPENDIX B: NUCLEATION OF VOIDS

Nucleation of voids in a material under irradiation is a process occurring as a result of diffusion *in the size space* of small nuclei of voids (vacancy clusters) which, while shrinking on average, occasionally reach the critical size. The time t_{nucl} required for a critical nucleus to form by diffusion of vacancy clusters in the size space can be estimated as

$$t_{\mathrm{nucl}} \sim n_{cr}^2/2D(n_{cr}), \tag{B1}$$

where $D(n)$ is the size-dependent diffusion coefficient describing Brownian motion of a vacancy cluster along the n-axis, where n is the number of vacancies in a cluster, and n_{cr} is the number of vacancies in a critical nucleus. Using the expression for this size-space diffusion coefficient $D(n) = 3n^{1/3}/2(3\Omega/4\pi)^{2/3}[D_v c_v + D_i c_i]$ given by Eq. 7 of Ref. 28, we find that

$$t_{\mathrm{nucl}} \approx \frac{(3\Omega/4\pi)^{2/3}n_{cr}^{5/3}}{3(D_v c_v + D_i c_i)}. \tag{B2}$$

Substituting into this equation the numerical values of $n_{cr}=50$, $\Omega = 10^{-23}$ cm^{-3}, and $D_v c_v + D_i c_i = 0.1$ μm^2/year (the latter value comes from the numerical solution of the reaction-diffusion model described above for $Kt = 10^{-2}$ NRT dpa) we find that $t_{\mathrm{nucl}} \sim 4.1\times 10^{-6}$ years. In the case where the irradiation rate is equal to $K=2$ NRT dpa/year our estimate shows that the kinetics of a nucleation event is characterized by the "dose" scale of the order of $Kt_{\mathrm{nucl}} \sim 10^{-5}$ NRT dpa. The fact that this value is many times smaller than the dose ($\geqslant 10^{-3}$ NRT dpa) at which experimental observations[13–15] were performed makes it possible to treat nucleation as a

sequence of events occurring instantaneously but continuously during the entire interval of observation. We can therefore introduce the probability of nucleating a void[28]

$$P = \sqrt{\frac{\beta}{6\pi R_{cr} n_{cr}} \frac{D_v c_v - D_i c_i}{(1 + n_{cr}^{1/3} d)}} \exp\left(- \frac{\eta(\beta/R_{cr}) n_{cr}^{2/3}}{1 + 1/(n_{cr}^{1/3} d)} \right), \tag{B3}$$

which is related to the nucleation rate ν entering Eq. (3) via $\nu = K(1-\epsilon_r)P/N_d$, where N_d is the average number of defects created in an individual collison cascade. In Eq. (B3) $d = 3(D_v c_v - D_i c_i)/2D_i c_i$ and $\beta = 2\gamma_s \Omega / k_B T$, where Ω is the atomic volume, γ_s is the coefficient of surface tension, and T is the absolute temperature. R_{cr} is the critical radius of a void given by[28]

$$R_{cr} = \beta / \ln[(D_v c_v - D_i c_i)/D_v c_\infty],$$

where $c_\infty = \exp[-E_f(\text{vac})/k_B T]$ and $n_{cr} = 4\pi R_{cr}^3 / 3\Omega$. Function $\eta(x)$ entering Eq. (B3) is related to the exponential integral function and is defined by

$$\eta(x) = \frac{(b_1 - a_1) + (b_2 - a_2)/x}{1 + b_1/x + b_2/x^2},$$

where $a_1 = 2.334733$, $b_1 = 3.330657$, $a_2 = 0.250621$, and $b_2 = 1.681534$.

*Electronic address: Sergei.Dudarev@UKAEA.org.uk

[1] K. Ehrlich, Philos. Trans. R. Soc. London, Ser. A **357**, 595 (1999); Fusion Eng. Des. **56/57**, 71 (2001).

[2] A. Möslang, K. Ehrlich, T. E. Shannon *et al.*, Nucl. Fusion **40**, 619 (2000).

[3] I. Cook, D. Ward, and S. L. Dudarev, Plasma Phys. Controlled Fusion **44**, B121 (2002).

[4] S. J. Zinkle and A. Kohyama, in *Proceedings of the 19th Symposium on Fusion Engineering*, January 21–25, 2002, Atlantic City (Baker and Taylor, New Jersey, 2002), pp. 477–483.

[5] G. R. Odette, B. D. Wirth, D. J. Bacon, and N. M. Ghoniem, MRS Bull. **26**, 176 (2001).

[6] G. Martin, Curr. Opin. Solid State Mater. Sci. **3**, 552 (1998).

[7] A. D. Brailsford and R. Bullough, J. Nucl. Mater. **44**, 121 (1972); Philos. Trans. R. Soc. London, Ser. A **302**, 87 (1981).

[8] L. K. Mansur, in *Kinetics of Inhomogeneous Processes*, edited by G. R. Freeman (Wiley, New York, 1987), Chap. 8.

[9] A. D. Brailsford, J. Nucl. Mater. **118**, 303 (1983).

[10] N. V. Doan and G. Martin, Phys. Rev. B **67**, 134107 (2003).

[11] M. Samaras, P. M. Derlet, H. Van Swygenhoven, and M. Victoria, Phys. Rev. Lett. **88**, 125505 (2002).

[12] S. G. Mayr and R. S. Averback, Phys. Rev. B **68**, 075419 (2003).

[13] B. N. Singh, T. Leffers, and A. Horswell, Philos. Mag. A **53**, 233 (1986).

[14] C. A. English, B. L. Eyre, and J. W. Muncie, Philos. Mag. A **56**, 453 (1987).

[15] B. N. Singh, A. Horswell, P. Toft, and D. J. Edwards, J. Nucl. Mater. **224**, 131 (1995).

[16] *Proceedings of the 11th International Conference on Fusion Reactor Materials (ICFRM-11), Kyoto, Japan, 2003*, edited by A. Kohyama, T. Muroga, A. Kimura, K. Abe, F. W. Wiffen, and R. E. Stoller, J. Nucl. Mater. **329–333**, 1 (2004).

[17] D. J. Bacon, A. F. Calder, and F. Gao, J. Nucl. Mater. **251**, 1 (1997).

[18] B. D. Wirth, G. R. Odette, D. Maroudas, and G. Lucas, J. Nucl. Mater. **244**, 185 (1997); **276**, 33 (2000).

[19] Yu. N. Osetsky, D. J. Bacon, A. Serra, B. N. Singh, and S. I. Golubov, J. Nucl. Mater. **276**, 65 (2000).

[20] M. Samaras, P. M. Derlet, H. Van Swygenhoven, and M. Victoria, Phys. Rev. B **68**, 224111 (2003).

[21] T. Leffers, B. N. Singh, A. V. Volobuyev, and V. V. Gann, Philos. Mag. A **53**, 243 (1986).

[22] H. Trinkaus, B. N. Singh, and A. J. E. Foreman, J. Nucl. Mater. **191**, 1 (1992); **206**, 200 (1993).

[23] M. Kiritani, J. Nucl. Mater. **251**, 237 (1997).

[24] H. Abe, N. Sekimura, and Y. Yang, J. Nucl. Mater. **323**, 220 (2003).

[25] W. Frank and A. Seeger, Mater. Sci. Forum **15/18**, 57 (1987).

[26] T S Hudson, S. L. Dudarev, and A P Sutton, Proc. R. Soc. London **A460**, 2457 (2004).

[27] T. S. Hudson, S. L. Dudarev, and A. P. Sutton, Proc. Ry. Soc. London, Ser. A (in press).

[28] A. A. Semenov and C. H. Woo, Phys. Rev. B **66**, 024118 (2002).

[29] C. H. Woo and B. N. Singh, Phys. Status Solidi B **159**, 609 (1990); Philos. Mag. A **65**, 889 (1992).

[30] M. C. Payne, M. P. Teter, D. C. Allan, T. A. Arias, and J. D. Joannopoulos, Rev. Mod. Phys. **64**, 1045 (1992).

[31] L.-M. Peng, S. L. Dudarev, and M. J. Whelan, *High-Energy Electron Diffraction and Microscopy* (Oxford University Press, New York, 2004) p. 64.

[32] M. Abramovitz and I. A. Stegun, *Handbook of Mathematical Functions* (Dover, NewYork, 1964) p. 231, Eq. 5.1.54.

[33] B. C. Skinner and C. H. Woo, Phys. Rev. B **30**, 3084 (1984).

[34] M. J. Norgett, M. T. Robinson, and I. M. Torrens, Nucl. Eng. Des. **33**, 50 (1975).

[35] A. A. Semenov and C. H. Woo, Appl. Phys. A: Mater. Sci. Process. **73**, 371 (2001).

[36] D. Walgraef, J. Lauzeral, and N. M. Ghoniem, Phys. Rev. B **53**, 14 782 (1996).

[37] B. N. Singh, M. Eldrup, A. Horswell, P. Ehrhart, and F. Dworschak, Philos. Mag. A **80**, 2629 (2000).